A Novel Model-Based MR Attenuation Correction Method for PET/MR Hybrid Imaging Considering Bone

Daniel H. Paulus[1]; Thomas Koesters[2,3]; Fernando Boada[2,3]; Kent P. Friedman[2]; Harald H. Quick[4,5]

[1] Institute of Medical Physics, Friedrich-Alexander-University Erlangen-Nürnberg (FAU), Erlangen, Germany
[2] Bernard and Irene Schwartz Center for Biomedical Imaging, Department of Radiology, New York University School of Medicine, New York, NY, USA
[3] Center for Advanced Imaging Innovation and Research (CAI2R), New York, NY, USA
[4] Erwin L. Hahn Institute for MR Imaging, University Duisburg-Essen, Essen, Germany
[5] High Field and Hybrid MR Imaging, University Hospital Essen, Essen, Germany

Introduction

Whole-body hybrid PET/MR imaging has become a fast-growing research field in medical imaging, especially since the introduction of the first integrated whole-body PET/MRI system in 2010 [1, 2]. With an increasing role in clinical routine, it allows simultaneous data acquisition of metabolic information by the means of PET and anatomical information with excellent soft tissue contrast and further functional imaging parameters by the means of MR.

For accurate and quantitative PET images, appropriate attenuation correction (AC) is required. In hybrid PET/CT systems, CT images providing tissue attenuation as Hounsfield units (HU) can directly be transformed to attenuation coefficient maps (μ-maps) given in linear attenuation coefficients (LACs) at 511 keV by using a bilinear conversion [3]. In PET/MR hybrid imaging, PET AC is more challenging [4], since MR images provide mainly proton densities and cannot directly be converted to LACs at 511 keV.

Over recent years, image segmentation-based methods, on the basis of a fast 3-dimensional (3D) MR Dixon sequence are being used for AC in routine PET/MR hybrid imaging. This method provides up to 4 tissue classes including air, fat, lung, and soft tissue [5] assigned with predefined LACs. A short acquisition time, easy implementation, and robust performance have led this method to be used for several clinical PET/MRI studies [6–8], albeit there are certain limitations compared to CT-based AC. A limited MR imaging field-of-view might lead to image truncations in the μ-map and bone is not recognized by the MR Dixon sequence. Thus, LACs of bone are set to the soft tissue value in 4-compartment methods leading to a potential

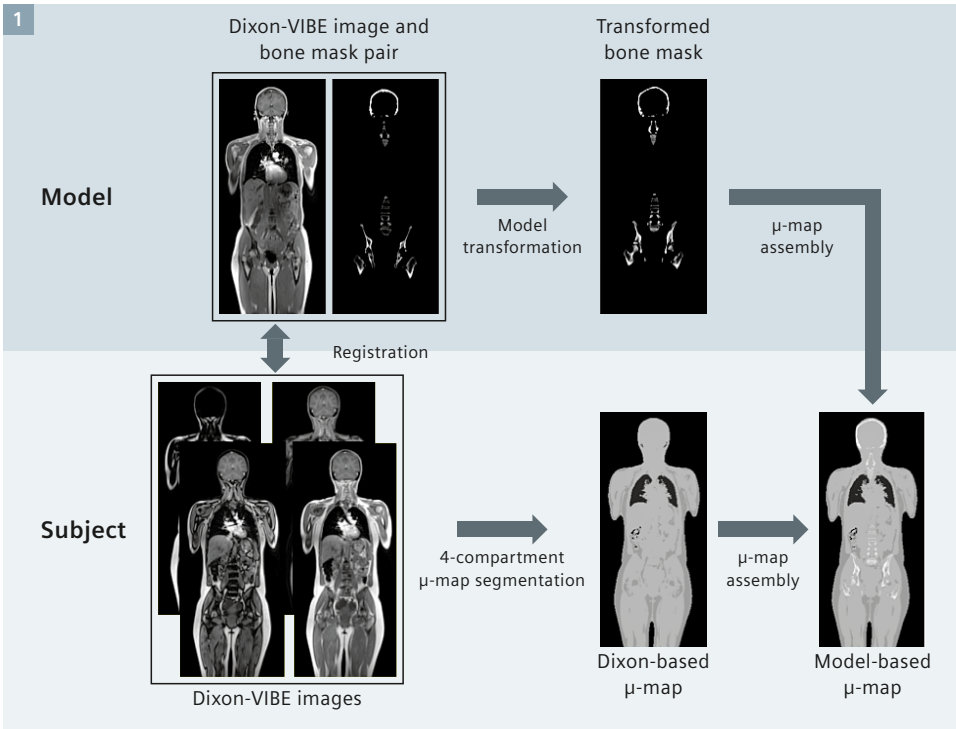

1 Schematic drawing of the novel model-based algorithm that considers bone in whole-body PET/MRI AC. The model (upper part) consists of a set of MR image and bone mask pairs that are registered to the subject's (lower part) Dixon-VIBE images for each body bone individually. The transformation is applied to the bone segmentation for each body bone and added to the 4-compartment segmentation-based μ-map at all voxels of densities higher than soft tissue.

underestimation of PET standard uptake values (SUVs). This effect has been quantitatively evaluated by several groups and an SUV bias between -6.5% and -11.2% compared to CT AC was calculated for bone lesions [5, 9, 10]. However, all of the cited studies were based on PET/CT data sets, and CT images have been modified by thresholding to simulate a segmentation-based MR µ-map, before transforming to LACs at 511 keV.

For simultaneous PET/MR imaging of the head and brain new approaches have been proposed to include cortical bone information in the MR-based µ-map, such as atlas registration and pattern recognition [11] or pseudo CTs generated with an ultrashort echo time MR sequence [12]. These methods, however, have not yet been assigned to routine whole-body PET/MR imaging.

A novel prototype model-based AC method for PET/MR hybrid imaging has recently been introduced that considers major bones besides the head to improve whole-body PET/MRI AC [13]. In this study [13] the new method was compared to both the routine Dixon-based AC and the CT-based AC, and all reconstructions were based on only the PET/MRI raw data. This excludes inter-scanner biases that might otherwise occur, if PET raw data sets of different PET systems are used in quantitative comparisons. In this article, which is based on the study by Paulus et al. [13], the new model-based method is described and PET/MRI patient cases are demonstrated and quantitatively evaluated showing the benefit of adding cortical bone to the segmentation-based µ-map.

Materials and methods

Study population

This study was approved by the institutional review and ethical board. 20 patients (mean age, 54.8 ± 16.8 y, range 25–85 y, 19 female) first underwent a clinically indicated PET/CT examination (Biograph mCT, Siemens Healthcare, Knoxville, TN, USA) according to the standard clinical protocol, followed by a subsequent whole-body PET/MRI acquisition (Biograph mMR, Siemens Healthcare, Erlangen, Germany). MR/PET data sets were acquired on a Biograph mMR under the auspices of a NYU Langone Medical Center IRB approved-protocol. Written informed consent was obtained from all patients and no additional radiotracer was injected for the PET/MRI acquisition. An average activity of 541.7 ± 18.4 MBq was injected[1] and the PET/MRI acquisitions were performed 200.3 ± 48.8 min post injection. 14 patients were examined for 5 bed positions and 6 patients were examined for 3 bed positions where the head was not included into the PET/MRI protocol.

PET/MRI µ-maps

All PET reconstructions are based on emission data acquired with the PET/MRI system using identical parameters, like scanner hardware and identical reconstruction settings. Three different µ-maps were used for the PET reconstructions of each subject.

- **Standard MR-based µ-map**
  The routine MR-based segmentation AC (Dixon) was performed with a breath-hold 2-point 3D Dixon-VIBE (volume interpolated breath-hold examination) technique. The µ-map provides 4 different tissue classes including air, fat, lung, and soft tissue and was acquired with standard protocol parameters: Matrix 192 x 126 with 128 slices (coronal orientation); voxel size (2.60 x 2.60) mm², slice thickness 3.12 mm, TR = 3.6 ms, TE = 2.46 ms, flip angle 10°, and acquisition time 19 s per bed position.
- **Model-based µ-map**
  The novel method (Model), illustrated in Figure 1 is based on the regular 4-compartment segmentation from a Dixon sequence. Bone information is added to these µ-maps by using a model-based prototype bone segmentation algorithm[2] (Siemens Healthcare, Erlangen, Germany) [13] using continuous LACs for bone in cm^{-1} at the PET energy level of 511 keV. The model consists of the major body bones including left and right

[1] The full prescribing information for the Fludeoxyglucose F^{18} injection can be found at page 91.

[2] The product is still under development and not commercially available yet. Its future availability cannot be ensured.

2

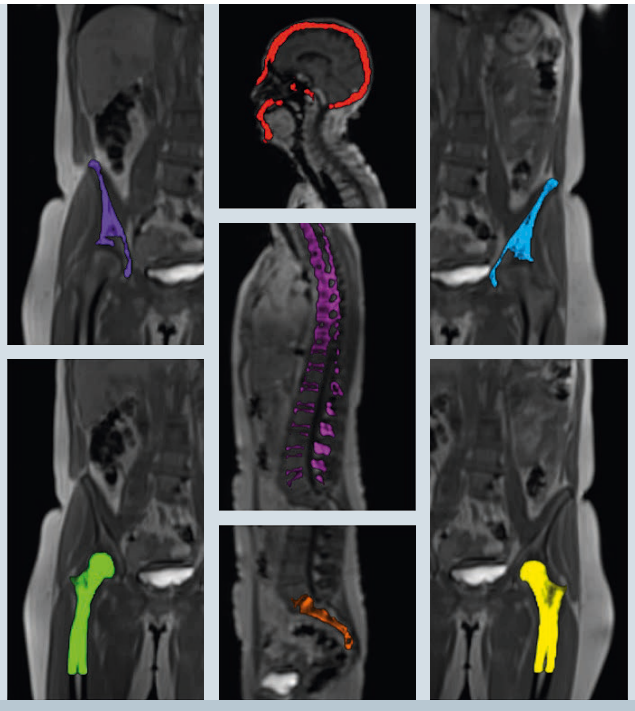

2 An illustration of the major bones containing bone densities as continuous LACs in cm^{-1} at 511 keV used in the model-based AC. The bone information is superimposed with the subject's MR image demonstrating exact anatomical registration.

femur (upper part), left and right hip, spine (including sacrum), and skull (Fig. 2) with a corresponding pre-aligned MR image. At each major body bone, the MR image of the model is individually registered with the subject MR image.

The first step of the model algorithm is a learning-based approach to detect a set of landmarks surrounding each bone [14]. Subsequently, a more sophisticated deformable registration [15] is performed to bring the model to the subject space more precisely. Following the same transformations, the pre-aligned bone masks containing LAC in cm^{-1} are then brought to the subject space and added to the original Dixon-based µ-map at all voxels of densities higher than soft tissue. The average running time of the algorithm was between 2 and 3 minutes per whole-body data set.

- **CT-based µ-map**
  As a standard of reference quantification, CT-based AC (CT) was performed with the PET/MRI emission data. CT images derived from the PET/CT data of the same subject were non-rigidly registered to the anatomical Dixon-VIBE images and visually compared to ensure optimal anatomical alignment. The two-step registration framework was similar to the algorithm used for the Model method. It consists of a landmark-based rigid registration [14] and a deformable registration [15]. The CT images were transformed using the standard bilinear conversion [3] to provide LACs at 511 keV. Since PET/CT acquisitions were performed with patient's arms up and not with arms down as in PET/MRI, the arms were removed in the CT-based image and replaced with arm information of the Dixon-based µ-map.

Data processing
All µ-maps were post-processed with a maximum likelihood reconstruction of attenuation and activity (MLAA) algorithm [16] to add missing parts mainly of the arms. All PET images were reconstructed iteratively on the PET/MRI system with a 3D ordinary Poisson ordered-subsets expectation maximization (OP-OSEM) algorithm using 3 iterations and 21 subsets. The standard whole-body PET/MRI reconstruction parameters were used: Image matrix 172 x 172, pixel size 4.173 x 4.173 mm^2, slice thickness 2.031 mm, Gaussian filtering 4 mm.

PET image analysis
PET images were superimposed with the corresponding MR images of a radial T1-weighted VIBE sequence used for MRI diagnosis in whole-body PET/MRI acquisitions. Based on the MR image, volumes of interest (VOIs) were manually drawn on normal tissue and the mean SUV (SUV_{mean}) was calculated for following regions: aorta/blood level, liver, spleen, femoral head left/right, iliac bones left/right, psoas muscles left/right, 3rd lumbar vertebra (L3), and subcutaneous fat. Additionally, VOIs of all identified soft-tissue lesions as well as bone lesions of all 20 subjects were drawn using a 50% maximum contour of the PET SUV. The CT-based reconstruction of each subject was used as the standard of reference.

The VOIs of one femoral head and one iliac bone of two patients were excluded from the analysis due to hip implants and resulting MR image artifacts. Furthermore, one femoral head VOI and two iliac bone VOIs were excluded due to lesions or metastases inside the VOIs. One spleen VOI is missing, since the patient underwent a splenectomy.

Results

Figure 3 shows all three different µ-maps of one subject in coronal view. The additional bone information that is added to the Dixon-based µ-map is illustrated in Figure 4.

The difference of background VOIs within all 20 patients depends very much on the tissue type. For soft tissue including aorta, liver, spleen, subcutaneous fat, and psoas muscles, the difference of the SUV_{mean} compared to CT is 2.4% for Dixon and 2.7% for Model. Cold-background VOIs of bony tissue were underestimated with Dixon by -46.5% ± 9.3% (femoral head), -20.0% ± 5.5% (iliac

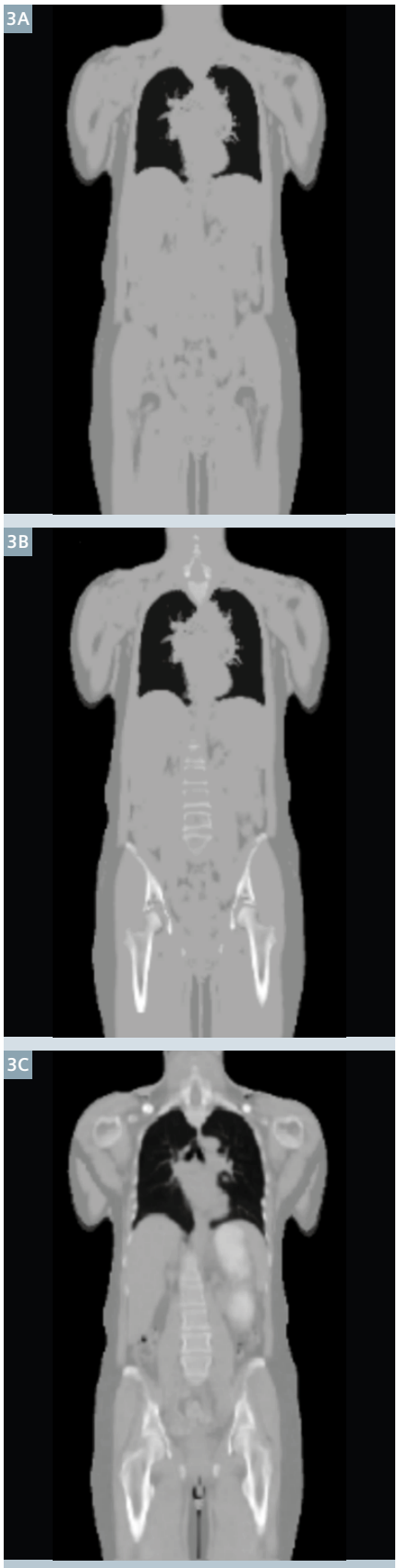

3 Dixon **(3A)**, Model **(3B)**, and CT **(3C)** µ-map exemplarily shown for one patient.

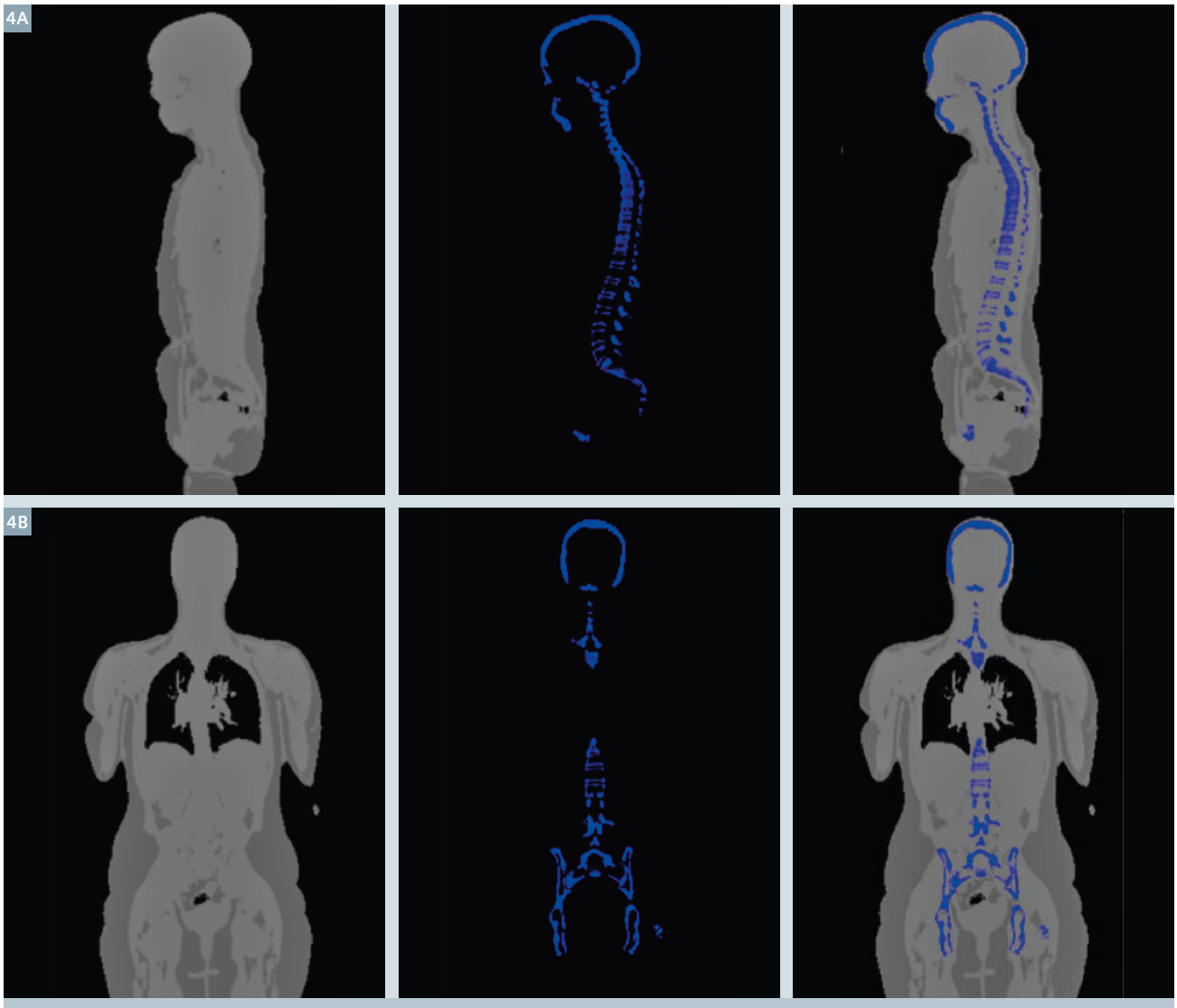

4 Dixon-based segmentation µ-map (left), bone mask information (middle) and combined model-based µ-map (right) of one subject in sagittal **(4A)** and coronal **(4B)** view.

bones), and -9.9% ± 8.9% (L3). The bias is reduced with the new Model method to -4.9% ± 7.7% (femoral heads), -2.8% ± 4.6% (iliac bones), and -7.1% ± 7.8% (L3).

The SUV deviation between Dixon and Model is negligible for soft tissue lesions with a mean of 0.3% and a maximum of 1.5%. Compared to the CT-based AC, the deviation is 5.1% ± 5.1% and 5.2 ± 5.2% for the Dixon method and the Model method, respectively. In this way, lung lesions are excluded, where the segmentation µ-map differs from the CT µ-map in terms of LACs.

For bone lesions an underestimation of -7.3% ± 5.3% was calculated for Dixon compared to CT, which is reduced to -2.9% ± 5.8% with the new Model method.

Figures 5 to 7 show the radial T1-weighted VIBE sequence used for MRI diagnosis, the PET image, and the superimposed PET/MR image of three different patients with bone lesions. The SUV comparison shows the improvement regarding PET quantification in bone lesions as a result of adding bone information to the Dixon segmentation-based µ-map. Case 1 has a spinous process bone metastasis showing an SUV_{mean} of 4.15 for the CT AC. The deviations with Dixon AC and Model AC compared to CT AC are -5.1% and -1.4%, respectively. Case 2 shows a bone metastasis in the right femoral head with an SUV of 5.51. The deviation of the SUV_{mean} with Dixon AC and Model AC compared to CT AC is -11.3% and -1.5%, respectively. In case 3, iliac bone metastases with a calculated SUV of 7.03 (right) and 8.99 (left) have been evaluated. The deviation of the SUV_{mean} with Dixon AC and Model AC compared to CT AC was -10.7% and -6.1% for the right side, respectively, and -10.8% and -5.0% for the left side, respetively.

5

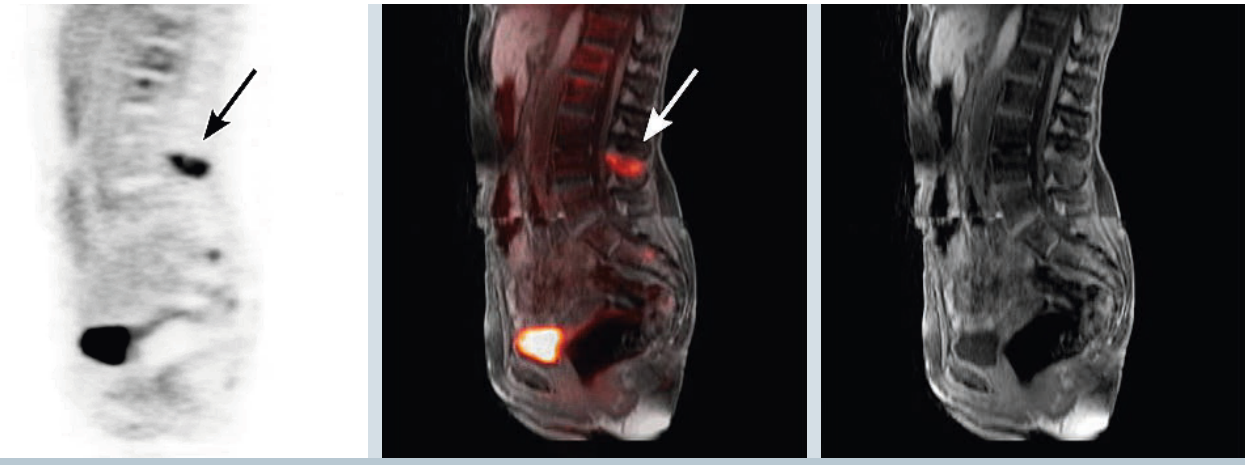

5 Sagittal PET image, superimposed PET/MR image, and diagnostic MR image of the radial T1-weighted VIBE sequence, showing a spinous process bone metastasis. The deviation of the SUV_{mean} with Dixon AC and Model AC compared to CT AC was -5.1% and -1.4%, respectively.

6

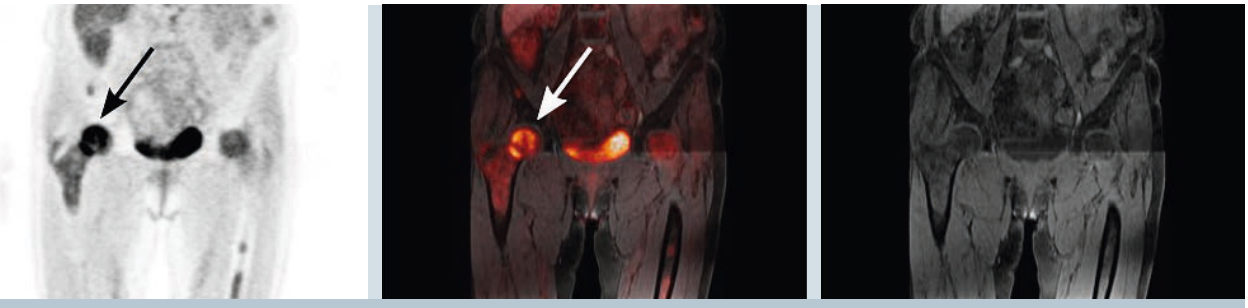

6 Coronal PET image, superimposed PET/MR image, and diagnostic MR image of the radial T1-weighted VIBE sequence, showing a bone metastasis in the right femoral head. The deviation of the SUV_{mean} with Dixon AC and Model AC compared to CT AC was -11.3% and -1.5%, respectively.

7

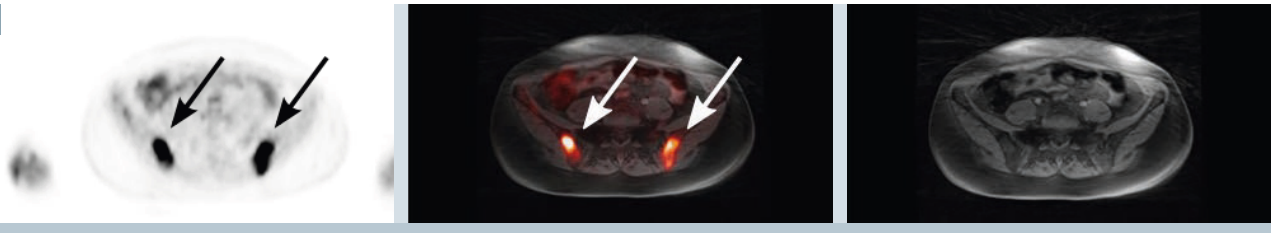

7 Transaxial PET image, superimposed PET/MR image, and diagnostic MR image of the radial T1-weighted VIBE sequence, showing iliac bone metastases (right and left). The deviation of the SUV_{mean} with Dixon AC and Model AC compared to CT AC was -10.7% and -6.1% for the right side, respectively, and -10.8% and -5.0% for the left side, respetively.

Discussion

On a dataset of 20 PET/MRI patients, it was shown that the new Model approach improved PET SUVs in bony regions when compared to CT-based AC and to Dixon MRI-based AC. The results of the study are comparable with previous whole-body hybrid imaging studies that have calculated an SUV underestimation for bony regions between -7% and -11% if bone is considered as soft tissue in the μ-map. The previous studies, however, were all based on PET/CT data [6, 10] and not PET/MRI data.

Unlike the relatively high impact in bony regions, the evaluation of SUVs of normal soft tissue shows that the Model as well as the Dixon approach have consistent results when compared to CT-based AC serving as standard of reference. This demonstrates the limited impact on SUVs in soft tissues that are not close to bone when corrected with μ-maps including bone information, as also shown by other groups [6, 13]. Furthermore, it shows that for these regions the routine Dixon μ-map performs virtually identically compared to the CT AC. This effect was also observable for soft tissue lesions.

The possibility should be considered that there are bone density variations in the same bone groups between patients. While the bias for patients without bone diseases is expected to be relatively small, bone density changes due to diseases might affect the PET quantification more. Due to abnormal decreased bone density SUVs might be overestimated in or near those bones, since LACs of the model are higher than the actual bone LACs. This however, remains true for most MRI-based AC methods including segmentation- and atlas-based AC. For better matching of bone densities, the model might be improved by grouping it into different ages, sex, and races.

In contrast to former whole-body PET/MRI AC studies, PET data of each patient within this study is based only on the emission raw data set of the PET/MRI system, which focuses the quantitative comparison to the differences of the μ-maps. Physiological aspects, like different patient positioning or tracer washout between PET/CT and PET/MRI scans, can therefore be excluded. The attenuation effect of local radiofrequency surface coils leading to a potential underestimation of -5% with a maximum up to -20% when neglected in AC [17,18] can also be excluded, since all PET reconstructions are performed with the same settings and raw data.

CT-based μ-maps of the body trunk were used as a standard of reference in this study. Due to the fact that patient positioning in PET/CT is performed with arms up, CT information of the patient arms was missing in these CT-based μ-maps. Since PET/MR imaging is performed with the arms resting beside the patient body, the MRI-based μ-maps contain the arms. Consequently, the missing information was added from the corresponding Dixon-based μ-map to the CT-based μ-map such that the different patient positioning (arms up vs. arms down) thus did not introduce additional bias. Furthermore, the effect of the arms for VOIs inside the body is expected to be small and is thus negligible.

The presented approach does not require any additional MRI sequences in the PET/MR imaging protocol, as needed in other methods such as the ultrashort echo time approach [12]. It is only based on the Dixon MRI sequence that is already acquired for the routine MRI-based AC. A data reconstruction run-time of about 2 to 3 minutes per whole-body case is short compared to other methods [11].

Conclusion

It is shown in 20 subjects that the new 5-compartment model improves the PET quantification compared to the current 4-compartment AC method, especially in bony tissue, bone lesions, and tissue close to bone. As the new method is based on the same Dixon MRAC acquisition, no additional scan time is required which is important given the generally long exam time of whole-body MR-PET scans.

Acknowledgments

This work was performed in collaboration with the Bernard and Irene Schwartz Center for Biomedical Imaging of New York University (NYU) and Siemens Healthcare GmbH. The authors would like to thank Matthias Fenchel, Christian Geppert, Yiqiang Zhan, Gerardo Hermosillo, and David Faul (all Siemens Healthcare GmbH) for their valuable participation and support.

References

1 Delso G, Furst S, Jakoby B, Ladebeck R, Ganter C, Nekolla SG, Schwaiger M, Ziegler SI. Performance measurements of the Siemens mMR integrated whole-body PET/MR scanner. J Nucl Med. 2011;52:1914–1922.
2 Quick HH. Integrated PET/MR. J Magn Reson Imaging. 2014;39:243-258.
3 Kinahan PE, Townsend DW, Beyer TT, Sashin D. Attenuation correction for a combined 3D PET/CT scanner. Med Phys. 1998;25:2046–2053.
4 Keereman V, Mollet P, Berker Y, Schulz V, Vandenberghe S. Challenges and current methods for attenuation correction in PET/MR. MAGMA. 2013;26:81–98.
5 Martinez-Moller A, Souvatzoglou M, Delso G, Bundschuh RA, Chefd'hotel C, Ziegler SI, Navab N, Schwaiger M, Nekolla SG. Tissue classification as a potential approach for attenuation correction in whole-body PET/MRI: evaluation with PET/CT data. J Nucl Med. 2009;50:520–526.
6 Drzezga A, Souvatzoglou M, Eiber M, Beer AJ, Fürst S, Martinez-Möller A, Nekolla SG, Ziegler S, Ganter C, Rummeny EJ, Schwaiger M. First clinical experience with integrated whole-body PET/MR: comparison to PET/CT in patients with oncologic diagnoses. J Nucl Med. 2012;53:845–855.
7 Wiesmüller M, Quick HH, Navalpakkam BK, Lell MM, Uder M, Ritt P, Schmidt D, Beck M, Kuwert T, von Gall CC. Comparison of lesion detection and quantitation of tracer uptake between PET from a simultaneously acquiring whole-body PET/MR hybrid scanner and PET from PET/CT. Eur J Nucl Med Mol Imaging. 2013;40:12–21.
8 Quick HH, von Gall CC, Zeilinger M, Wiesmüller M, Braun H, Ziegler S, Kuwert T, Uder M, Dörfler A, Kalender WA, Lell M. Integrated whole-body PET/MR hybrid imaging: clinical experience. Invest Radiol. 2013;48:280–289.
9 Samarin A, Burger C, Wollenweber SD, Crook DW, Burger IA, Schmid DT, von Schulthess GK, Kuhn FPPET/MR imaging of bone lesions--implications for PET quantification from imperfect attenuation correction. Eur J Nucl Med Mol Imaging. 2012;39:1154–1160.
10 Hofmann M, Bezrukov I, Mantlik F, Aschoff P, Steinke F, Beyer T, Pichler BJ, Schölkopf B. MRI-based attenuation correction for whole-body PET/MRI: quantitative evaluation of segmentation- and atlas-based methods. J Nucl Med. 2011;52:1392–1399.
11 Hofmann M, Steinke F, Scheel V, Charpiat G, Farquhar J, Aschoff P, Brady M, Bernhard Schölkopf B, Pichler BJ. MRI-based attenuation correction for PET/MRI: A novel approach combining pattern recognition and atlas registration. J Nucl Med. 2008;49:1875–1883.
12 Navalpakkam BK, Braun H, Kuwert T, Quick HH. Magnetic resonance-based attenuation correction for PET/MR hybrid imaging using continuous valued attenuation maps. Invest Radiol. 2013;48:323–332.
13 Paulus DH, Quick HH, Geppert C, Fenchel M, Zhan Y, Hermosillo G, Faul D, Boada F, Friedman KP, Koesters T. Whole-Body PET/MR Imaging: Quantitative Evaluation of a Novel Model-Based MR Attenuation Correction Method Including Bone. J Nucl Med. 2015;56:1061-1066.

14 Zhan Y, Zhou X, Peng Z, Krishnan A. Active scheduling of organ detection and segmentation in whole-body medical images. In: Metaxas D, Axel L, Fichtinger G, Székely G, eds. Medical Image Computing and Computer-Assisted Intervention–MICCAI 2008. Berlin, Germany: Springer; 2008:313–321.

15 Hermosillo G, Chefd'Hotel C, Faugeras O. Variational methods for multimodal image matching. Int J Comput Vis; 2002;50:329–343.

16 Nuyts J, Bal G, Kehren F, Fenchel M, Michel C, Watson C. Completion of a Truncated Attenuation Image From the Attenuated PET Emission Data. IEEE Trans Med Imaging. 2012;32:237–246.

17 Paulus DH, Braun H, Aklan B, Quick HH. Simultaneous PET/MR imaging: MR-based attenuation correction of local radiofrequency surface coils. Med Phys. 2012;39:4306–4315.

18 Kartmann R, Paulus DH, Braun H, Aklan B, Ziegler S, Navalpakkam BK, Lentschig M, Quick HH. Integrated PET/MR imaging: Automatic attenuation correction of flexible RF coils. Med Phys. 2013;40:082301.

Contact

Daniel H. Paulus, MSc
Institute of Medical Physics (IMP)
University of Erlangen-Nürnberg
Henkestr. 91, 91052 Erlangen,
Germany
daniel.paulus@imp.uni-erlangen.de

Contact

Prof. Harald H. Quick, Ph.D.
Director
Erwin L. Hahn Institute for MR Imaging
High Field and Hybrid MR-Imaging
University of Duisburg-Essen
Kokerei Zollverein
Kokereiallee 7, 45147 Essen, Germany
harald.quick@uni-due.de

HIGHLIGHTS OF PRESCRIBING INFORMATION

These highlights do not include all the information needed to use Fludeoxyglucose F 18 Injection safely and effectively. See full prescribing information for Fludeoxyglucose F 18 Injection.
Fludeoxyglucose F 18 Injection, USP
For intravenous use
Initial U.S. Approval: 2005

RECENT MAJOR CHANGES

Warnings and Precautions (5.1, 5.2)	7/2010
Adverse Reactions (6)	7/2010

INDICATIONS AND USAGE

Fludeoxyglucose F18 Injection is indicated for positron emission tomography (PET) imaging in the following settings:

- Oncology: For assessment of abnormal glucose metabolism to assist in the evaluation of malignancy in patients with known or suspected abnormalities found by other testing modalities, or in patients with an existing diagnosis of cancer.
- Cardiology: For the identification of left ventricular myocardium with residual glucose metabolism and reversible loss of systolic function in patients with coronary artery disease and left ventricular dysfunction, when used together with myocardial perfusion imaging.
- Neurology: For the identification of regions of abnormal glucose metabolism associated with foci of epileptic seizures (1).

DOSAGE AND ADMINISTRATION

Fludeoxyglucose F 18 Injection emits radiation. Use procedures to minimize radiation exposure. Screen for blood glucose abnormalities.

- In the oncology and neurology settings, instruct patients to fast for 4 to 6 hours prior to the drug's injection. Consider medical therapy and laboratory testing to assure at least two days of normoglycemia prior to the drug's administration (5.2).
- In the cardiology setting, administration of glucose-containing food or liquids (e.g., 50 to 75 grams) prior to the drug's injection facilitates localization of cardiac ischemia (2.3).

Aseptically withdraw Fludeoxyglucose F 18 Injection from its container and administer by intravenous injection (2).

The recommended dose:

- for adults is 5 to 10 mCi (185 to 370 MBq), in all indicated clinical settings (2.1).
- for pediatric patients is 2.6 mCi in the neurology setting (2.2).

Initiate imaging within 40 minutes following drug injection; acquire static emission images 30 to 100 minutes from time of injection (2).

DOSAGE FORMS AND STRENGTHS

Multi-dose 30mL and 50mL glass vial containing 0.74 to 7.40 GBq/mL (20 to 200 mCi/mL) Fludeoxyglucose F 18 Injection and 4.5mg of sodium chloride with 0.1 to 0.5% w/w ethanol as a stabilizer (approximately 15 to 50 mL volume) for intravenous administration (3).

CONTRAINDICATIONS

None

WARNINGS AND PRECAUTIONS

- Radiation risks: use smallest dose necessary for imaging (5.1).
- Blood glucose adnormalities: may cause suboptimal imaging (5.2).

ADVERSE REACTIONS

Hypersensitivity reactions have occurred; have emergency resuscitation equipment and personnel immediately available (6).
To report SUSPECTED ADVERSE REACTIONS, contact PETNET Solutions, Inc. at 877-473-8638 or FDA at 1-800-FDA-1088 or www.fda.gov/medwatch.

USE IN SPECIFIC POPULATIONS

Pregnancy Category C: No human or animal data. Consider alternative diagnostics; use only if clearly needed (8.1).

- Nursing mothers: Use alternatives to breast feeding (e.g., stored breast milk or infant formula) for at least 10 half-lives of radioactive decay, if Fludeoxyglucose F 18 Injection is administered to a woman who is breast-feeding (8.3).
- Pediatric Use: Safety and effectiveness in pediatric patients have not been established in the oncology and cardiology settings (8.4).

See 17 for PATIENT COUNSELING INFORMATION

Revised: 1/2011

FULL PRESCRIBING INFORMATION: CONTENTS*

* Sections or subsections omitted from the full prescribing information are not listed.

FULL PRESCRIBING INFORMATION

1 INDICATIONS AND USAGE

Fludeoxyglucose F 18 Injection is indicated for positron emission tomography (PET) imaging in the following settings:

1.1 Oncology

For assessment of abnormal glucose metabolism to assist in the evaluation of malignancy in patients with known or suspected abnormalities found by other testing modalities, or in patients with an existing diagnosis of cancer.

1.2 Cardiology

For the identification of left ventricular myocardium with residual glucose metabolism and reversible loss of systolic function in patients with coronary artery disease and left ventricular dysfunction, when used together with myocardial perfusion imaging.

1.3 Neurology

For the identification of regions of abnormal glucose metabolism associated with foci of epileptic seizures.

2 DOSAGE AND ADMINISTRATION

Fludeoxyglucose F 18 Injection emits radiation. Use procedures to minimize radiation exposure. Calculate the final dose from the end of synthesis (EOS) time using proper radioactive decay factors. Assay the final dose in a properly calibrated dose calibrator before administration to the patient [see Description (11.2)].

2.1 Recommended Dose for Adults

Within the oncology, cardiology and neurology settings, the recommended dose for adults is 5 to 10 mCi (185 to 370 MBq) as an intravenous injection.

2.2 Recommended Dose for Pediatric Patients

Within the neurology setting, the recommended dose for pediatric patients is 2.6 mCi, as an intravenous injection. The optimal dose adjustment on the basis of body size or weight has not been determined [see Use in Special Populations (8.4)].

2.3 Patient Preparation

- To minimize the radiation absorbed dose to the bladder, encourage adequate hydration. Encourage the patient to drink water or other fluids (as tolerated) in the 4 hours before their PET study.
- Encourage the patient to void as soon as the imaging study is completed and as often as possible thereafter for at least one hour.
- Screen patients for clinically significant blood glucose abnormalities by obtaining a history and/or laboratory tests [see Warnings and Precautions (5.2)]. Prior to Fludeoxyglucose F 18 PET imaging in the oncology and neurology settings, instruct patient to fast for 4 to 6 hours prior to the drug's injection.
- In the cardiology setting, administration of glucose-containing food or liquids (e.g., 50 to 75 grams) prior to Fludeoxyglucose F18 Injection facilitates localization of cardiac ischemia

2.4 Radiation Dosimetry

The estimated human absorbed radiation doses (rem/mCi) to a newborn (3.4 kg), 1-year old (9.8 kg), 5-year old (19 kg), 10-year old (32 kg), 15-year old (57 kg), and adult (70 kg) from intravenous administration of Fludeoxyglucose F 18 Injection are shown in Table 1. These estimates were calculated based on human[2] data and using the data published by the International Commission on Radiological Protection[4] for Fludeoxyglucose ^{18}F. The dosimetry data show that there are slight variations in absorbed radiation dose for various organs in each of the age groups. These dissimilarities in absorbed radiation dose are due to developmental age variations (e.g., organ size, location, and overall metabolic rate for each age group). The identified critical organs (in descending order) across all age groups evaluated are the urinary bladder, heart, pancreas, spleen, and lungs.

Table 1. Estimated Absorbed Radiation Doses (rem/mCi) After Intravenous Administration of Fludeoxyglucose F-18 Injection[a]

Organ	Newborn (3.4 kg)	1-year old (9.8 kg)	5-year old (19 kg)	10-year old (32 kg)	15-year old (57 kg)	Adult (70 kg)
Bladder wall[b]	4.3	1.7	0.93	0.60	0.40	0.32
Heart wall	2.4	1.2	0.70	0.44	0.29	0.22
Pancreas	2.2	0.68	0.33	0.25	0.13	0.096
Spleen	2.2	0.84	0.46	0.29	0.19	0.14
Lungs	0.96	0.38	0.20	0.13	0.092	0.064
Kidneys	0.81	0.34	0.19	0.13	0.089	0.074
Ovaries	0.80	0.8	0.19	0.11	0.058	0.053
Uterus	0.79	0.35	0.19	0.12	0.076	0.062
LLI wall *	0.69	0.28	0.15	0.097	0.060	0.051
Liver	0.69	0.31	0.17	0.11	0.076	0.058
Gallbladder wall	0.69	0.26	0.14	0.093	0.059	0.049
Small intestine	0.68	0.29	0.15	0.096	0.060	0.047
ULI wall **	0.67	0.27	0.15	0.090	0.057	0.046
Stomach wall	0.65	0.27	0.14	0.089	0.057	0.047
Adrenals	0.65	0.28	0.15	0.095	0.061	0.048
Testes	0.64	0.27	0.14	0.085	0.052	0.041
Red marrow	0.62	0.26	0.14	0.089	0.057	0.047
Thymus	0.61	0.26	0.14	0.086	0.056	0.044
Thyroid	0.61	0.26	0.13	0.080	0.049	0.039
Muscle	0.58	0.25	0.13	0.078	0.049	0.039
Bone surface	0.57	0.24	0.12	0.079	0.052	0.041
Breast	0.54	0.22	0.11	0.068	0.043	0.034
Skin	0.49	0.20	0.10	0.060	0.037	0.030
Brain	0.29	0.13	0.09	0.078	0.072	0.070
Other tissues	0.59	0.25	0.13	0.083	0.052	0.042

[a] MIRDOSE 2 software was used to calculate the radiation absorbed dose. Assumptions on the biodistribution based on data from Gallagher et al.1 and Jones et al.2

[b] The dynamic bladder model with a uniform voiding frequency of 1.5 hours was used. *LLI = lower large intestine; **ULI = upper large intestine

2.5 Radiation Safety – Drug Handling

- Use waterproof gloves, effective radiation shielding, and appropriate safety measures when handling Fludeoxyglucose F 18 Injection to avoid unnecessary radiation exposure to the patient, occupational workers, clinical personnel and other persons.
- Radiopharmaceuticals should be used by or under the control of physicians who are qualified by specific training and experience in the safe use and handling of radionuclides, and whose experience and training have been approved by the appropriate governmental agency authorized to license the use of radionuclides.
- Calculate the final dose from the end of synthesis (EOS) time using proper radioactive decay factors. Assay the final dose in a properly calibrated dose calibrator before administration to the patient [see Description (11.2)].
- The dose of Fludeoxyglucose F 18 used in a given patient should be minimized consistent with the objectives of the procedure, and the nature of the radiation detection devices employed.

2.6 Drug Preparation and Administration

- Calculate the necessary volume to administer based on calibration time and dose.
- Aseptically withdraw Fludeoxyglucose F 18 Injection from its container.
- Inspect Fludeoxyglucose F 18 Injection visually for particulate matter and discoloration before administration, whenever solution and container permit.
- Do not administer the drug if it contains particulate matter or discoloration; dispose of these unacceptable or unused preparations in a safe manner, in compliance with applicable regulations.
- Use Fludeoxyglucose F 18 Injection within 12 hours from the EOS.

2.7 Imaging Guidelines

- Initiate imaging within 40 minutes following Fludeoxyglucose F 18 Injection administration.
- Acquire static emission images 30 to 100 minutes from the time of injection.

3 DOSAGE FORMS AND STRENGTHS

Multiple-dose 30 mL and 50 mL glass vial containing 0.74 to 7.40 GBq/mL (20 to 200 mCi/mL) of Fludeoxyglucose F 18 Injection and 4.5 mg of sodium chloride with 0.1 to 0.5% w/w ethanol as a stabilizer (approximately 15 to 50 mL volume) for intravenous administration.

4 CONTRAINDICATIONS

None

5 WARNINGS AND PRECAUTIONS

5.1 Radiation Risks

Radiation-emitting products, including Fludeoxyglucose F 18 Injection, may increase the risk for cancer, especially in pediatric patients. Use the smallest dose necessary for imaging and ensure safe handling to protect the patient and health care worker [see Dosage and Administration (2.5)].

5.2 Blood Glucose Abnormalities

In the oncology and neurology setting, suboptimal imaging may occur in patients with inadequately regulated blood glucose levels. In these patients, consider medical therapy and laboratory testing to assure at least two days of normoglycemia prior to Fludeoxyglucose F 18 Injection administration.

6 ADVERSE REACTIONS

Hypersensitivity reactions with pruritus, edema and rash have been reported in the postmarketing setting. Have emergency resuscitation equipment and personnel immediately available.

7 DRUG INTERACTIONS

The possibility of interactions of Fludeoxyglucose F 18 Injection with other drugs taken by patients undergoing PET imaging has not been studied.

8 USE IN SPECIFIC POPULATIONS

8.1 Pregnancy

Pregnancy Category C

Animal reproduction studies have not been conducted with Fludeoxyglucose F 18 Injection. It is also not known whether Fludeoxyglucose F 18 Injection can cause fetal harm when administered to a pregnant woman or can affect reproduction capacity. Consider alternative diagnostic tests in a pregnant woman; administer Fludeoxyglucose F 18 Injection only if clearly needed.

8.3 Nursing Mothers

It is not known whether Fludeoxyglucose F 18 Injection is excreted in human milk. Consider alternative diagnostic tests in women who are breast-feeding. Use alternatives to breast feeding (e.g., stored breast milk or infant formula) for at least 10 half-lives of radioactive decay, if Fludeoxyglucose F 18 Injection is administered to a woman who is breast-feeding.

8.4 Pediatric Use

The safety and effectiveness of Fludeoxyglucose F 18 Injection in pediatric patients with epilepsy is established on the basis of studies in adult and pediatric patients. In pediatric patients with epilepsy, the recommended dose is 2.6 mCi. The optimal dose adjustment on the basis of body size or weight has not been determined. In the oncology or cardiology settings, the safety and effectiveness of Fludeoxyglucose F 18 Injection have not been established in pediatric patients.

11 DESCRIPTION

11.1 Chemical Characteristics

Fludeoxyglucose F 18 Injection is a positron emitting radiopharmaceutical that is used for diagnostic purposes in conjunction with positron emission tomography (PET) imaging. The active ingredient 2-deoxy-2-[^{18}F]fluoro-D-glucose has the molecular formula of $C_6H_{11}{}^{18}FO_5$ with a molecular weight of 181.26, and has the following chemical structure:

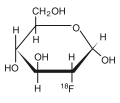

Fludeoxyglucose F 18 Injection is provided as a ready to use sterile, pyrogen free, clear, colorless solution. Each mL contains between 0.740 to 7.40GBq (20.0 to 200 mCi) of 2-deoxy-2-[^{18}F]fluoro-D-glucose at the EOS, 4.5 mg of sodium chloride and 0.1 to 0.5% w/w ethanol as a stabilizer. The pH of the solution is between 4.5 and 7.5. The solution is packaged in a multiple-dose glass vial and does not contain any preservative.

11.2 Physical Characteristics

Fluorine F 18 decays by emitting positron to Oxygen O 16 (stable) and has a physical half-life of 109.7 minutes. The principal photons useful for imaging are the dual 511 keV gamma photons, that are produced and emitted simultaneously in opposite direction when the positron interacts with an electron (Table 2).

Table 2. Pricipal Radiation Emission Data for Fluorine F18

Radiation/Emission	% Per Disintegration	Mean Energy
Positron (b+)	96.73	249.8 keV
Gamma (±)*	193.46	511.0 keV

*Produced by positron annihilation

From: Kocher, D.C. Radioactive Decay Tables DOE/TIC-I 1026, 89 (1981)

The specific gamma ray constant (point source air kerma coefficient) for fluorine F 18 is 5.7 R/hr/mCi (1.35 x 10-6 Gy/hr/kBq) at 1 cm. The half-value layer (HVL) for the 511 keV photons is 4 mm lead (Pb). The range of attenuation coefficients for this radionuclide as a function of lead shield thickness is shown in Table 3. For example, the interposition of an 8 mm thickness of Pb, with a coefficient of attenuation of 0.25, will decrease the external radiation by 75%.

Table 3. Radiation Attenuation of 511 keV Photons by lead (Pb) shielding

Shield thickness (Pb) mm	Coefficient of attenuation
0	0.00
4	0.50
8	0.25
13	0.10
26	0.01
39	0.001
52	0.0001

For use in correcting for physical decay of this radionuclide, the fractions remaining at selected intervals after calibration are shown in Table 4.

Table 4. Physical Decay Chart for Fluorine F18

Minutes	Fraction Remaining
0*	1.000
15	0.909
30	0.826
60	0.683
110	0.500
220	0.250

*calibration time

12 CLINICAL PHARMACOLOGY

12.1 Mechanism of Action

Fludeoxyglucose F 18 is a glucose analog that concentrates in cells that rely upon glucose as an energy source, or in cells whose dependence on glucose increases under pathophysiological conditions. Fludeoxyglucose F 18 is transported through the cell membrane by facilitative glucose transporter proteins and is phosphorylated within the cell to [18F] FDG-6-phosphate by the enzyme hexokinase. Once phosphorylated it cannot exit until it is dephosphorylated by glucose-6-phosphatase. Therefore, within a given tissue or pathophysiological process, the retention and clearance of Fludeoxyglucose F 18 reflect a balance involving glucose transporter, hexokinase and glucose-6-phosphatase activities. When allowance is made for the kinetic differences between glucose and Fludeoxyglucose F 18 transport and phosphorylation (expressed as the ‚lumped constant" ratio), Fludeoxyglucose F 18 is used to assess glucose metabolism. In comparison to background activity of the specific organ or tissue type, regions of decreased or absent uptake of Fludeoxyglucose F 18 reflect the decrease or absence of glucose metabolism. Regions of increased uptake of Fludeoxyglucose F 18 reflect greater than normal rates of glucose metabolism.

12.2 Pharmacodynamics

Fludeoxyglucose F 18 Injection is rapidly distributed to all organs of the body after intravenous administration. After background clearance of Fludeoxyglucose F 18 Injection, optimal PET imaging is generally achieved between 30 to 40 minutes after administration.

In cancer, the cells are generally characterized by enhanced glucose metabolism partially due to (1) an increase in activity of glucose transporters, (2) an increased rate of phosphorylation activity, (3) a reduction of phosphatase activity or, (4) a dynamic alteration in the balance among all these processes. However, glucose metabolism of cancer as reflected by Fludeoxyglucose F 18 accumulation shows considerable variability. Depending on tumor type, stage, and location, Fludeoxyglucose F 18 accumulation may be increased, normal, or decreased. Also, inflammatory cells can have the same variability of uptake of Fludeoxyglucose F 18.

In the heart, under normal aerobic conditions, the myocardium meets the bulk of its energy requirements by oxidizing free fatty acids. Most of the exogenous glucose taken up by the myocyte is converted into glycogen. However, under ischemic conditions, the oxidation of free fatty acids decreases, exogenous glucose becomes the preferred myocardial sub strate, glycolysis is stimulated, and glucose taken up by the myocyte i s metabolized immediately instead of being converted into glycogen. Under these conditions, phosphorylated Fludeoxyglucose F 18 accumulates in the myocyte and can be detected with PET imaging.

In the brain, cells normally rely on aerobic metabolism. In epilepsy, the glucose metabolism varies. Generally, during a seizure, glucose metabolism increases. Interictally, the seizure focus tends to be hypometabolic.

12.3 Pharmacokinetics

Distribution: In four healthy male volunteers, receiving an intravenous administration of 30 seconds in duration, the arterial blood level profile for Fludeoxyglucose F 18 decayed triexponentially. The effective half-life ranges of the three phases were 0.2 to 0.3 minutes, 10 to 13 minutes with a mean and standard deviation (STD) of 11.6 (±) 1.1 min, and 80 to 95 minutes with a mean and STD of 88 (±) 4 min.

Plasma protein binding of Fludeoxyglucose F 18 has not been studied.

Metabolism: Fludeoxyglucose F 18 is transported into cells and phosphorylated to [^{18}F]-FDG-6- phosphate at a rate proportional to the rate of glucose utilization within that tissue. [F18]-FDG-6-phosphate presumably is metabolized to 2-deoxy-2-[F18]fluoro-6-phospho-D-mannose([F 18]FDM-6-phosphate).

Fludeoxyglucose F 18 Injection may contain several impurities (e.g., 2-deoxy-2-chloro-D-glucose (ClDG)). Biodistribution and metabolism of ClDG are presumed to be similar to Fludeoxyglucose F 18 and would be expected to result in intracellular formation of 2-deoxy-2-chloro-6-phospho-D-glucose (ClDG-6-phosphate) and 2-deoxy-2-chloro-6-phospho-D-mannose (ClDM-6-phosphate). The phosphorylated deoxyglucose compounds are dephosphorylated and the resulting compounds (FDG, FDM, ClDG, and ClDM) presumably leave cells by passive diffusion. Fludeoxyglucose F 18 and related compounds are cleared from non-cardiac tissues within 3 to 24 hours after administration. Clearance from the cardiac tissue may require more than 96 hours. Fludeoxyglucose F 18 that is not involved in glucose metabolism in any tissue is then excreted in the urine.

Elimination: Fludeoxyglucose F 18 is cleared from most tissues within 24 hours and can be eliminated from the body unchanged in the urine. Three elimination phases have been identified in the reviewed literature. Within 33 minutes, a mean of 3.9% of the administrated radioactive dose was measured in the urine. The amount of radiation exposure of the urinary bladder at two hours post-administration suggests that 20.6% (mean) of the radioactive dose was present in the bladder.

Special Populations:

The pharmacokinetics of Fludeoxyglucose F 18 Injection have not been studied in renally-impaired, hepatically impaired or pediatric patients. Fludeoxyglucose F 18 is eliminated through the renal system. Avoid excessive radiation exposure to this organ system and adjacent tissues.

The effects of fasting, varying blood sugar levels, conditions of glucose intolerance, and diabetes mellitus on Fludeoxyglucose F 18 distribution in humans have not been ascertained [see Warnings and Precautions (5.2)].

13 NONCLINICAL TOXICOLOGY

13.1 Carcinogenesis, Mutagenesis, Impairment of Fertility

Animal studies have not been performed to evaluate the Fludeoxyglucose F 18 Injection carcinogenic potential, mutagenic potential or effects on fertility.

14 CLINICAL STUDIES

14.1 Oncology

The efficacy of Fludeoxyglucose F 18 Injection in positron emission tomography cancer imaging was demonstrated in 16 independent studies. These studies prospectively evaluated the use of Fludeoxyglucose F 18 in patients with suspected or known malignancies, including non-small cell lung cancer, colo-rectal, pancreatic, breast, thyroid, melanoma, Hodgkin's and non-Hodgkin's lymphoma, and various types of metastatic cancers to lung, liver, bone, and axillary nodes. All these studies had at least 50 patients and used pathology as a standard of truth. The Fludeoxyglucose F 18 Injection doses in the studies ranged from 200 MBq to 740 MBq with a median and mean dose of 370 MBq.

In the studies, the diagnostic performance of Fludeoxyglucose F 18 Injection varied with the type of cancer, size of cancer, and other clinical conditions. False negative and false positive scans were observed. Negative Fludeoxyglucose F 18 Injection PET scans do not exclude the diagnosis of cancer. Positive Fludeoxyglucose F 18 Injection PET scans can not replace pathology to establish a diagnosis of cancer. Non-malignant conditions such as fungal infections, inflammatory processes and benign tumors have patterns of increased glucose metabolism that may give rise to false-positive scans. The efficacy of Fludeoxyglucose F 18 Injection PET imaging in cancer screening was not studied.

14.2 Cardiology

The efficacy of Fludeoxyglucose F 18 Injection for cardiac use was demonstrated in ten independent, prospective studies of patients with coronary artery disease and chronic left ventricular systolic dysfunction who were scheduled to undergo coronary revascularization. Before revascularization, patients underwent PET imaging with Fludeoxyglucose F 18 Injection (74 to 370 MBq, 2 to 10 mCi) and perfusion imaging with other diagnostic radiopharmaceuticals. Doses of Fludeoxyglucose F 18 Injection ranged from 74 to 370 MBq (2 to 10 mCi). Segmental, left ventricular, wall-motion assessments of asynergic areas made before revascularization were compared in a blinded manner to assessments made after successful revascularization to identify myocardial segments with functional recovery.

Left ventricular myocardial segments were predicted to have reversible loss of systolic function if they showed Fludeoxyglucose F 18 accumulation and reduced perfusion (i.e., flow-metabolism mismatch). Conversely, myocardial segments were predicted to have irreversible loss of systolic function if they showed reductions in both Fludeoxyglucose F 18 accumulation and perfusion (i.e., matched defects).

Findings of flow-metabolism mismatch in a myocardial segment may suggest that successful revascularization will restore myocardial function in that segment. However, false-positive tests occur regularly, and the decision to have a patient undergo revascularization should not be based on PET findings alone. Similarly, findings of a matched defect in a myocardial segment may suggest that myocardial function will not recover in that segment, even if it is successfully revascularized. However, false-negative tests occur regularly, and the decision to recommend against coronary revascularization, or to recommend a cardiac transplant, should not be based on PET findings alone. The reversibility of segmental dysfunction as predicted with Fludeoxyglucose F 18 PET imaging

depends on successful coronary revascularization. Therefore, in patients with a low likelihood of successful revascularization, the diagnostic usefulness of PET imaging with Fludeoxyglucose F 18 Injection is more limited.

14.3 Neurology

In a prospective, open label trial, Fludeoxyglucose F 18 Injection was evaluated in 86 patients with epilepsy. Each patient received a dose of Fludeoxyglucose F 18 Injection in the range of 185 to 370 MBq (5 to 10 mCi). The mean age was 16.4 years (range: 4 months to 58 years; of these, 42 patients were less than 12 years and 16 patients were less than 2 years old). Patients had a known diagnosis of complex partial epilepsy and were under evaluation for surgical treatment of their seizure disorder. Seizure foci had been previously identified on ictal EEGs and sphenoidal EEGs. Fludeoxyglucose F 18 Injection PET imaging confirmed previous diagnostic findings in 16% (14/87) of the patients; in 34% (30/87) of the patients, Fludeoxyglucose F 18 Injection PET images provided new findings. In 32% (27/87), imaging with Fludeoxyglucose F 18 Injection was inconclusive. The impact of these imaging findings on clinical outcomes is not known.

Several other studies comparing imaging with Fludeoxyglucose F 18 Injection results to subsphenoidal EEG, MRI and/or surgical findings supported the concept that the degree of hypometabolism corresponds to areas of confirmed epileptogenic foci. The safety and effectiveness of Fludeoxyglucose F 18 Injection to distinguish idiopathic epileptogenic foci from tumors or other brain lesions that may cause seizures have not been established.

15 REFERENCES

1. Gallagher B.M., Ansari A., Atkins H., Casella V., Christman D.R., Fowler J.S., Ido T., MacGregor R.R., Som P., Wan C.N., Wolf A.P., Kuhl D.E., and Reivich M. "Radiopharmaceuticals XXVII. 18F-labeled 2-deoxy-2-fluoro-d-glucose as a radiopharmaceutical for measuring regional myocardial glucose metabolism in vivo: tissue distribution and imaging studies in animals," J Nucl Med, 1977; 18, 990-6.
2. Jones S.C., Alavi, A., Christman D., Montanez, I., Wolf, A.P., and Reivich M. "The radiation dosimetry of 2 [F-18] fluoro-2-deoxy-D-glucose in man," J Nucl Med, 1982; 23, 613-617.
3. Kocher, D.C. "Radioactive Decay Tables: A handbook of decay data for application to radiation dosimetry and radiological assessments," 1981, DOE/TIC-I 1026, 89.
4. ICRP Publication 53, Volume 18, No. I-4,1987, pages 75-76.

16 HOW SUPPLIED/STORAGE AND DRUG HANDLING

Fludeoxyglucose F 18 Injection is supplied in a multi-dose, capped 30 mL and 50 mL glass vial containing between 0.740 to 7.40 GBq/mL (20 to 200 mCi/mL), of no carrier added 2-deoxy-2-[F 18] fluoro-D-glucose, at end of synthesis, in approximately 15 to 50 mL. The contents of each vial are sterile, pyrogen-free and preservative-free.

NDC 40028-511-30; 40028-511-50

Receipt, transfer, handling, possession, or use of this product is subject to the radioactive material regulations and licensing requirements of the U.S. Nuclear Regulatory Commission, Agreement States or Licensing States as appropriate.

Store the Fludeoxyglucose F 18 Injection vial upright in a lead shielded container at 25°C (77°F); excursions permitted to 15-30°C (59-86°F).

Store and dispose of Fludeoxyglucose F 18 Injection in accordance with the regulations and a general license, or its equivalent, of an Agreement State or a Licensing State.

The expiration date and time are provided on the container label. Use Fludeoxyglucose F 18 Injection within 12 hours from the EOS time.

17 PATIENT COUNSELING INFORMATION

Instruct patients in procedures that increase renal clearance of radioactivity.

Encourage patients to:

- drink water or other fluids (as tolerated) in the 4 hours before their PET study.
- void as soon as the imaging study is completed and as often as possible thereafter for at least one hour.

Manufactured by: PETNET Solutions Inc.
810 Innovation Drive
Knoxville, TN 37932

Distributed by: PETNET Solutions Inc.
810 Innovation Drive
Knoxville, TN 37932

PETNET Solutions

PN0002262 Rev. A

March 1, 2011

Indications

Fludeoxyglucose F^{18} Injection is indicated for positron emission tomography (PET) imaging in the following settings:

- **Oncology:** For assessment of abnormal glucose metabolism to assist in the evaluation of malignancy in patients with known or suspected abnormalities found by other testing modalities, or in patients with an existing diagnosis of cancer.
- **Cardiology:** For the identification of left ventricular myocardium with residual glucose metabolism and reversible loss of systolic function in patients with coronary artery disease and left ventricular dysfunction, when used together with myocardial perfusion imaging.
- **Neurology:** For the identification of regions of abnormal glucose metabolism associated with foci of epileptic seizures.

Important Safety Information

- **Radiation Risks:** Radiationemitting products, including Fludeoxyglucose F^{18} Injection, may increase the risk for cancer, especially in pediatric patients. Use the smallest dose necessary for imaging and ensure safe handling to protect the patient and healthcare worker.
- **Blood Glucose Abnormalities:** In the oncology and neurology setting, suboptimal imaging may occur in patients with inadequately regulated blood glucose levels. In these patients, consider medical therapy and laboratory testing to assure at least two days of normoglycemia prior to Fludeoxyglucose F^{18} Injection administration.
- **Adverse Reactions:** Hypersensitivity reactions with pruritus, edema and rash have been reported; have emergency resuscitation equipment and personnel immediately available.